Towards arm tremor diagnosis

Mohamed Elgendi[1] Flavien Picon[2] Nadia Magnenat-Thalmann[2]
Derek Abbott[3]

[1]Department of Computing Science, University of Alberta, Canada
[2]Institute of Media Innovation, Nanyang Technological University, Singapore
[3]School of Electrical and Electronic Engineering, University of Adelaide, Australia

July 18, 2013

Abstract

Many clinical studies have shown that the arm movement of patients with neurological injury is often slow. In this paper, the speed analysis of arm movement is presented, with the aim of evaluating arm movement automatically using a Kinect camera. The consideration of arm movement appears trivial at first glance, but in reality it is very complex neural and biomechanical process that can potentially be used for detecting a neurological disorder. This is a preliminary study, on healthy subjects, which investigates three different arm-movement speeds: fast, medium and slow. With a sample size of 27 subjects, our developed algorithm is able to classify the three different speed classes (slow, normal, and fast) with overall error of 5.43% for interclass speed classification and 0.49% for interaclass classification. This is the first step towards enabling future studies that investigate abnormality in arm movement, via use of a Kinect camera.

Introduction

According to the World Health Organization, essential tremor affects an estimated 10 million people in the United States [1, 2]. Essential tremor is the most common adult movement disorder, and is as much as 20 times more prevalent than Parkinson's disease [2, 3]. Essential tremor is traditionally viewed as a progressive neurological disorder that causes involuntary shaking of particular parts of the body, usually the head and hands [4]. However, the most recognizable feature is a tremor of the arms or hands that is apparent during voluntary movements such as eating and writing [5]. Although essential tremor is often mild, patients with severe tremor have difficulty performing many of their daily routine activities [6, 7]. Essential tremor usually causes slowness in body-parts movement, which is more salient in the hand. Slowness in arm movement is also common in many other disorders, such as Huntington's chorea [8], Parkinson's

disease [9] and cerebellar diseases [10]. However the abnormality in arm movement varies from one disease to another. Given the vast array of disorders associated with abnormal movements, the challenge for the rehabilitation community is in obtaining high quality evaluations at low cost.

Recently, Kinect cameras offer an extremely inexpensive and effective tool for tracking body movements that is very promising for the investigation of tremor and slowness in arm movement [11]. To our knowledge, there are no studies that investigate the speed of arm-movement joints for detecting abnormality in arm movements using Kinect or any other depth cameras. However, several arm-movement recognition systems have considered the speed as a feature. Min et al. [12] confirmed that arm-movement recognition is usually dependent on the trajectory of arm movement, and that position, speed, and curvature are useful features. Campbell et al. [13] investigated ten different features for arm-movement recognition using a Hidden Markov Model (HMM). They indicated that speed features are superior to positional features. Yoon et al. [14] used hand speed as an important feature for arm-movement recognition.

Other researchers estimated the speed of arm-movement using an accelerometer, for example Rehm et al. [15] used the power of the accelerometer as a feature to classify the arm movement into low and high speed regimes. In contrast to those studies, in this paper we systematically explore the speed of arm-movement joints, with the aim of improving the classification of the arm-movement speed. Our study builds upon Rehm's work by providing a device-free analysis of arm movement, exploring the impact of different joints on the overall arm movement, and validating the system in a noisy environment.

Materials and Methods

Ethics Statement

In this study, no film recordings of subjects were made. The Kinect camera outputs numerical data that directly relate to hand movements. Only de-indentified numerical data, representing motion vectors, are stored on the database. Volunteers are researchers at office of the Institute for Media Innovation, NTU, Singapore. All data is available at: `http://www3.ntu.edu.sg/imi/piconflavien/autres/data-speed-arm.zip` and `http://www.elgendi.net/databases.htm`.

Data Collection

There are currently no standard Kinect databases for arm-movement analysis available to evaluate our developed algorithm. However, the Institute of Media Innovation at Nanyang Technological University has one database that contains arm movement data of 27 healthy volunteers (6 females and 21 males); with a mean $\pm$ SD age of 29.7 $\pm$ 4.1, height of 172.9 $\pm$ 9.3, arm length of 71.3 $\pm$ 5.2. Two of them were left-handed. The motions were measured using the Kinect camera located 2.7 meters away from the subject at a height of 1.2 meters above the floor, cf. Figure 1. All Kinect data is acquired

using the Microsoft Kinect SDK Beta 1 (Microsoft, 2012) at a sampling frequency of 30 Hz. The Kinect device consists of laser light source, color camera and an infrared camera. The infrared laser source and the infrared video camera form the depth camera function, while the colour video camera provides colour data to the depth map. The technology was developed by PrimeSense (Tel-Aviv, Israel) and is disclosed in detail in their patents [16].

During the experiment, the body of the subject faces the sensor with an angle of 45° to the right of the Kinect sensor (as seen in Figure 1). The reason behind the 45° angle is to prevent the arm joints from intersecting with the body joints, as shown in Figure 2. This will generate reliable arm motion in order to study the impact of each joint of the arm on the overall speed of the right arm movement more precisely. These collected arm movements are used as a benchmark for effective speed detection of an arm movement. Measurements were taken with each subject standing vertical, with an initial position where both arms extended along the body side. Then, the subject is asked to raise a right arm up. Each subject performs three sets of trials: 'slow', 'normal', and 'fast'; with five arm movements for each set. Therefore the number of recorded movements is 405 (27 subjects $\times$ 5 movements $\times$ 3 speeds).

For the slow movement, the subject is instructed to raise an arm as if there is a heavy weight being lifted to simulate a typical indicator of Bradykinesia (a symptom of nervous system disorders, particularly Parkinson's disease). On the other hand, the fast arm movement indicates healthy motion, while the normal speed represents an average condition. Capture of the arm movement is carried out manually. In other words, the subjects wait for a signal from the recording person to start their movement and then they maintain their arm up until they get a signal to come back to the initial position. Each recording is played back, checked, and annotated as being in one of three classes 'slow', 'normal', or 'fast'. Two independent annotators annotated the speed category of each recorded movement; when two annotators disagree, the result is discarded and the subject is asked to repeat the experiment. The annotations were stored in a file to be compared automatically later with the speed features that will be discussed in the next section.

Methodology

The proposed arm-movement classification type algorithm consists of three main stages: pre-processing (resultant of coordinates as instantaneous velocity and low-pass filtering), feature extraction (calculating the first and second derivative and their mean and standard deviation) and classification (thresholding). The structure of the algorithm is shown in Figure 3.

Pre-Processing

The Kinect body tracking software API provides the real-time position of the body joints of each user [17]. Even though we focus mainly on the skeletal joints of the arm we chose to record the positions of all skeletal joints: center of gravity or legs movements are also

potential speed indicators. With 20 joints and 3 floating point values (real numbers) representing the x, y, z positions for each joint, each motion frame is expressed as a 60-element vector. The recorded joints cover all parts of the body but we focus mainly on the arm joints: shoulder, elbow, wrist and hand. Since the features only rely on the dynamics of the motion there are no differences in processing data from the left or right arm. Therefore we may process data from the joints of each subject's dominant arm (25 right-handed and 2 left-handed).

The 3D position (x, y, z) of a joint is expressed in the coordinate system of the Kinect and the units are meters [18]. Again, the selected features rely on motion dynamics so our system is view-independent: we do not have to express the positions in the coordinate system of the subject's body. The dynamic of each joint is computed using the variation of position of the joint over time. In the first step, each joint motion, sequence of 3D positions, is replaced by the distance between each frame as in Eq. 1. In Figure 2, the x, y, z coordinates are the positions vectors of a particular joint that vary 0 to n; where n is the number of frames in a performed motion. The instantaneous velocity of motion for a particular joint are calculated as the resultant of x, y, z positions over all frames that represents a motion. The instantaneous velocity (u_{inst}) for a given 3D motion is computed as follows:

$$u_{\text{inst}}[n] = \left.\frac{dx, y, z}{dt}\right|_{t=nT} = \frac{1}{T}\sqrt{(x[n] - x[n-1])^2 + (y[n] - y[n-1])^2 + (z[n] - z[n-1])^2}, \tag{1}$$

where T is the sampling interval and equals the reciprocal of the sampling frequency, and n is the number of motion data points.

As shown in Figure 4, the informative part of the motion lies below 6 Hz for all joints with different speed types. Thus, a low-pass filter has been applied. A first order, zero-phase bidirectional, Butterworth low-pass filter with cutoff frequency of 6 Hz is implemented. Figure 5, shows an example of the original data u_{inst}, at top-left, and the filtered data (V_{inst}), at top-right, with no phase distortion. Note that the low frequencies will play a major role in identifying hand movement speed, and ultimately hand tremors. The first order filter has been selected to avoid over-smoothing the acquired motion. This has been carried out empirically to find a condition where the substantial part of the motion is preserved while sensor errors were strongly reduced. We decided to record the raw data, i.e. without using the pre-defined filter provided in the Kinect SDK. By doing so, we have more control over the data analysis. We then have freedom to examine the affect of filtering on the classification rate.

Feature Extraction

Before continuing the discussion of the joint signals, it is important to know what features can be extracted from a hand movement first. In the literature, the instantaneous velocity and acceleration have been used in diagnosing arm movements. Almeida et al. [19] examined individuals with Parkinson's disease through the analysis of the upper-limb movement at different movement frequencies, and with different external timing

conditions using the instantaneous velocity. However, Helsen et al. [20] used the instantaneous velocity and acceleration to investigate the movements of the finger, elbow, and shoulder during a speed aiming movements. In this paper, two features are investigated: the instantaneous velocity and acceleration. The mathematical definition of the instantaneous velocity (u_{inst}) in 3D motion before filtering is described in Eq. 1, while the instantaneous acceleration (A_{inst}) is defined as:

$$A_{\text{inst}}[n] = \left.\frac{dV_{\text{inst}}}{dt}\right|_{t=nT} = \frac{1}{T}(V_{\text{inst}}[n] - V_{\text{inst}}[n-1]). \quad (2)$$

Although the Kinect camera has received increasing attention recently, it nevertheless suffers from noise, low resolution sensors, lack of color information, and occlusion problems [21]. Therefore, it is crucial that we filter the signal to improve the classification accuracy, especially if the main goal is to determine the speed type. In our study, we computed the instantaneous velocity and instantaneous acceleration for each arm joint. Then, we extracted the following features: average (mean) and standard deviation (SD). Figure 5 demonstrates the signal shape of four different joints of a arm movement based on the instantaneous velocity and acceleration. This is particularly interesting as it confirms that joints of a same limb have the same dynamics, especially for the hand and wrist signals. As the variance of the hand and wrist joint signals are quite higher compared to the elbow and shoulder signals, it is expected that the hand or the wrist signal would score higher accuracy in the classification of arm movements.

Classification

In this section, we check the linear velocity separability (based on the annotated files) over the calculated features in both filtered and non-filtered signals. Each motion contains a category parameter that was defined during the recording. We use this classification parameter to compare with the results of the feature classification. We perform inter subject classification: the process consists in 1) compute the feature value for each motion, 2) sort the motions based on the selected feature 3) compute the classification accuracy by counting the number of misclassified motions over total number of motions. For automated speed-type detection, two classifiers have been run in order to specify the exact value of the thresholds. The first classifier is fast/medium against slow, while the second classifier is fast against medium/slow. Figure 6 demonstrates the thresholds determination for inter- and intera -class speed classification. The two valleys reflect the thresholds that will be used for training the automatic speed detection. For example, in case of interaclass speed classification, the slow-medium threshold is 0.73 while the medium-fast threshold is 1.67 in non-filtered condition as shown in Figure 6 (top-left).

Results

The statistical Kruskal-Wallis and ANOVA tests allow us to investigate whether the hand-movement speed feature takes different values among the three speed classes. Low

p-values indicate large difference in the medians of the three speed classes for the Kruskal-Wallis test, while low p-values indicate large difference in the means of the three speed classes in the case of the ANOVA test. Both tests find that the three hand-movement speeds are significantly different, as the p-values were less than 0.05 in the case of filtered and non-filtered features. The very small p-value indicates that differences between the three speed classes are highly significant.

In Table 1, as expected, the hand joint was successfully classified into different speed types with the lowest error rate (0.49% for non-intra classification and 1.48% for inter classification). This result confirms the observation, shown in Figure 5, which is that the the mean of the instantaneous velocity for the hand motion contains more information compared to the other three joints in both cases filtered and un-filtered data. As can be seen, the hand joint is the most reliable for detecting speed in arm movement. It is interesting to note that features based on standard deviation perform better than those based on mean. Interestingly, the results of filtered and non-filtered hand-joint signal are relatively close. However, the filtered hand-joint signal scored a slightly lower classification error compared to the non-filtered signal.

Is it possible to predict the speed type before the completion of a full hand movement? To answer this, we investigated the percentage of the hand-movement from the start of the motion that contributes the most to the classification error. The results of this investigation are shown in Figure 7. For the interclassification, the first 50% of the hand instantaneous velocity provides classification error 18.7% and 8.8% for both features mean and SD, respectively. While in case of interaclass speed classification, the error rate scored by the first 60% was 4.4% for the mean and 7.4% for the standard deviation of the hand instantaneous velocity, without filtering. This is an interesting observation as the first 50% of a motion provides low classification error and relatively close in terms of performance to the whole motion. Knowing this fact can lead to an effective prediction, which can be even done in realtime without waiting for the whole motion to be completed. What portion of a hand-movement signal contributes the most to the classification error? Which 10% portion of the motion's signal contains the most useful information to distinguish the speed types?

Figure 8 shows the error rate for a sequential 10% of the motion signals. It can be seen, in the case of interclass speed classification; the portion 50–60% of the mean of the hand instantaneous velocity provides the lowest error rate of 6.4%. This is intuitive as the beginning of motion is the phase where the subjects is reaching a certain poses. Moreover, the interaclass analysis shows that a 0% error rate can be achieved if the 50–60% portion of the mean of the instantaneous velocity is used, instead of the whole hand movement. This confirms that the main characteristics of a motion is determined within 50–60%, and can be used for analysis or/and prediction.

Limitations of Study and Future Work

We recommend that future work examine our method on patients that suffer from hand tremor as the thresholds calculated in this study are based on healthy subjects. However,

mimicking unhealthy motion provides intial values for the system before assessing real patients at a hospital/clinic. A larger sample size and a diverse set of tremor movements are needed in order to generalize the findings of this study. To our knowledge, there is no available Kinect database measured from patients with hand tremor. In future studies it may be advisable to test the optimal distance for positioning Kinect as sometimes subjects cannot be detected if they are relatively close to the camera. It would be also useful to know how accurately the Kinect can estimate speed of arm movement compared the speed of arm movement with a benchmark standard (such as three dimensional analysis system, e.g. Vicon, optotrak, etc.). Technically, exploring simple features such as the mean and standard deviation of a motion is promising in terms of computational complexity and efficiency. However, this can be further improved by investigating other features in time and frequency domain.

Conclusion

In this paper we presented a speed analysis of arm movement. Results show that: 1) the instantaneous velocity provides more reliable classification compared to the instantaneous acceleration, 2) the mean is a better feature compared to the standard deviation for the instantaneous velocity, and 3) the hand joint is the most efficient joints for speed detection in an arm motion. Moreover, a low-pass filter improves the interclass speed classification but has no effect on the intraclass classification. For interclass speed classification, the mean of non-filtered instantaneous velocity scored 0.49% error rate in detecting the speed type over 405 motions; while the standard deviation of filtered instantaneous velocity scored 5.43% during the interaclass classification. Moreover, the first 60% provides a classification error relatively close to the use of a whole motion, can be used for predicting the speed type in realtime. Furthermore, the most important 10% of a whole motion is the 50–60%. The results are promising and this approach can be implemented in a human-computer-interaction system for interactive tremor diagnosis, specifically measuring hand-related disability and improvement. In our approach we asked healthy subjects to mimic abnormality by moving slowly, however testing this approach on patients with Parkinson's disease or any hand tremors remains as a task for future work.

Acknowledgments

This research, which is carried out at BeingThere Centre, is supported by the Singapore National Research Foundation under its International Research Centre @ Singapore Funding Initiative and administered by the IDM Programme Office.

References

[1] Paris-Robidas S, Brochu E, Sintes M, Emond V, Bousquet M, et al. (2012) Defective dentate nucleus GABA receptors in essential tremor. Brain 135: 105–116.

[2] Louis ED, Ferreira JJ (2010) How common is the most common adult movement disorder? Update on the worldwide prevalence of essential tremor. Movement Disorders 25: 534–541.

[3] Martinelli P, Rizzo G, Manners D, Tonon C, Pizza F, et al. (2007) Diffusion-weighted imaging study of patients with essential tremor. Movement Disorders 22: 1182–1185.

[4] Deuschl G, Bain P, Brin M (1998) Consensus statement of the movement disorder society on tremor. Movement Disorders 13: 2–23.

[5] Benito-León J, Louis ED (2007) Clinical update: diagnosis and treatment of essential tremor. The Lancet 369: 1152–1154.

[6] Bain PG, Mally J, Gresty M, Findley LJ (1993) Assessing the impact of essential tremor on upper limb function. Journal of Neurology 241: 54–61.

[7] Louis ED, Barnes L, Albert SM, Cote L, Schneier FR, et al. (2001) Correlates of functional disability in essential tremor. Movement Disorders 16: 914–920.

[8] Bittenbender J, Quadfasel F (1962) Rigid and akinetic forms of Huntington's chorea. Archives of Neurology 7: 275-288.

[9] Jahanshahi M, Jenkins IH, Brown RG, Marsden CD, Passingham RE, et al. (1995) Self-initiated versus externally triggered movements I. an investigation using measurement of regional cerebral blood flow with pet and movement-related potentials in normal and Parkinson's disease subjects. Brain 118: 913–933.

[10] Deuschl G, Wenzelburger R, Löffler K, Raethjen J, Stolze H (2000) Essential tremor and cerebellar dysfunction clinical and kinematic analysis of intention tremor. Brain 123: 1568–1580.

[11] Nguyen HA, Auvinet E, Mignotte M, de Guise JA, Meunier J (2012) Analyzing gait pathologies using a depth camera. In: 2012 Annual International Conference of the IEEE Engineering in Medicine and Biology Society (EMBC). pp. 4835–4838.

[12] Min BW, Yoon HS, Soh J, Yang YM, Ejima T (1997) Hand gesture recognition using hidden Markov models. In: 1997 IEEE International Conference on Systems, Man, and Cybernetics. volume 5, pp. 4232–4235.

[13] Campbell LW, Becker DA, Azarbayejani A, Bobick AF, Pentland A (1996) Invariant features for 3-D gesture recognition. In: Proceedings of the Second International Conference on Automatic Face and Gesture Recognition. pp. 157–162.

[14] Yoon HS, Soh J, Bae YJ, Yang HS (2001) Hand gesture recognition using combined features of location, angle and velocity. Pattern Recognition 34: 1491–1501.

[15] Rehm M, Bee N, André E (2008) Wave like an Egyptian: accelerometer based gesture recognition for culture specific interactions. In: HCI 2008 Culture, Creativity, Interaction. pp. 13–22.

[16] Arieli Y, Freedman B, Machline M, Shpunt A (2010) Depth Mapping Using Projected Patterns. US Patent: US20100118123 A1.

[17] Microsoft (2011). Kinect for windows SDK beta. URL `http://www.microsoft.com/en-us/kinectforwindows/`.

[18] Microsoft (2012). MSDN Library: Coordinate spaces.

[19] Almeida QJ, Wishart LR, Lee TD (2002) Bimanual coordination deficits with Parkinson's disease: the influence of movement speed and external cueing. Movement Disorders 17: 30–37.

[20] Helsen WF, Elliott D, Starkes JL, Ricker KL (2000) Coupling of eye, finger, elbow, and shoulder movements during manual aiming. Journal of Motor Behavior 32: 241–248.

[21] Baak A, Müller M, Bharaj G, Seidel HP, Theobalt C (2013) A data-driven approach for real-time full body pose reconstruction from a depth camera. In: Consumer Depth Cameras for Computer Vision, Springer. pp. 71–98.

[22] Hunter J. Matplotlib. URL `http://matplotlib.sourceforge.net/`.

Tables

Table 1: **Error rates for non-filtered and filtered arm-movement signals.** SD is the standard deviation; V_{inst} is the instantaneous velocity where A_{inst} is the instantaneous acceleration. Filtering is achieved using a Butterworth low-pass filter with a cutoff frequency of 6 Hz.

		Hand				**Wrist**			
		V_{inst}		A_{inst}		V_{inst}		A_{inst}	
		Mean error(%)	SD error(%)	Mean error(%)	SD error(%)	Mean error(%)	SD error(%)	Mean error(%)	er
Intra	**Non-filtered**	0.49	0.98	58.27	24.69	1.48	4.44	55.80	
	Filtered	0.49	2.46	58.27	11.35	1.48	4.44	55.80	
Inter	**Non-filtered**	8.39	6.41	60.74	30.86	10.37	12.34	58.02	
	Filtered	8.39	5.43	60.74	22.71	10.86	9.38	58.02	
		Elbow				**Shoulder**			
		V_{inst}		A_{inst}		V_{inst}		A_{inst}	
		Mean error(%)	SD error(%)	Mean error(%)	SD error(%)	Mean error(%)	SD error(%)	Mean error(%)	er
Intra	**Non-filtered**	1.48	6.41	53.82	21.72	4.44	11.60	36.04	
	Filtered	1.48	5.18	53.82	11.85	4.44	11.85	36.04	
Inter	**Non-filtered**	11.35	17.53	51.60	34.32	27.40	31.35	38.51	
	Filtered	11.35	14.56	51.60	27.90	27.40	31.11	38.51	

Figures

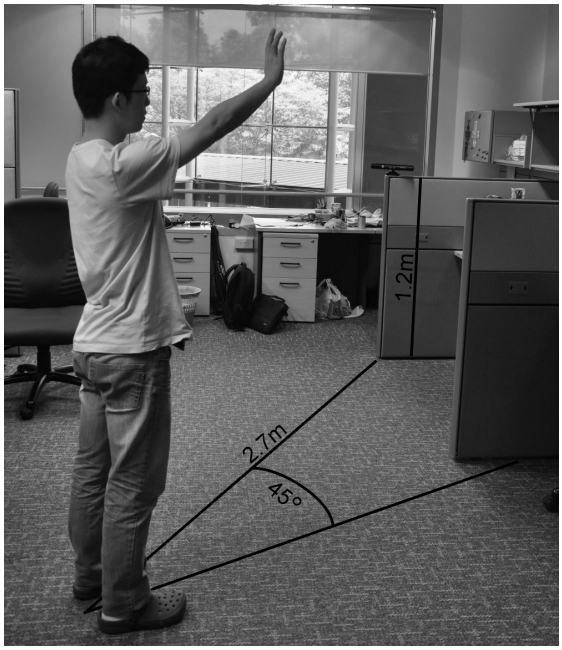

Figure 1: **Experimental Setup: the user is facing the camera at angle of 45° to the right of the sensor.** Every arm movement is recorded at fixed 2.7 m distance from the camera; where the camera is placed at height of 1.2 m above the floor.

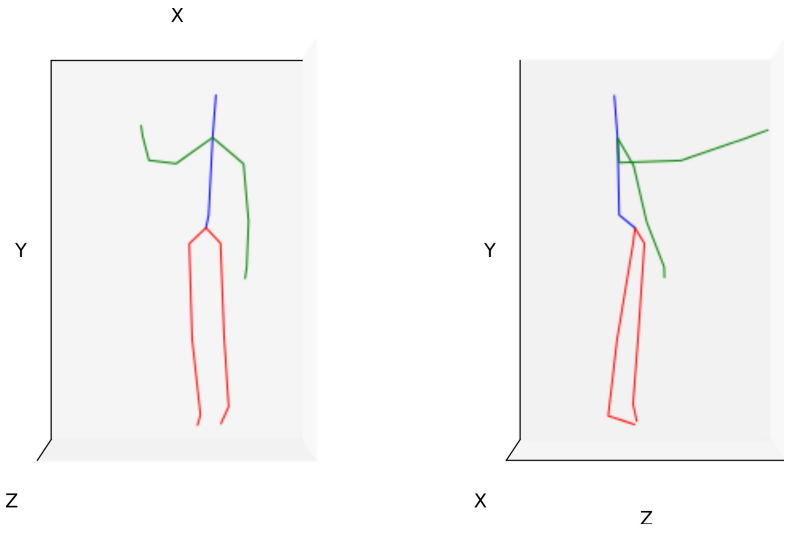

Figure 2: **Front and lateral view, of a subject, computed from the sensor data.** This plot represents the middle of the motion and was traced using Python 2.7 and the plotting module Matplotlib 1.1.0 [22]. The instantaneous velocity will be calculated using the x, y, z coordinates shown in the figure. The green lines represent arms, red represents legs and blue represents the torso.

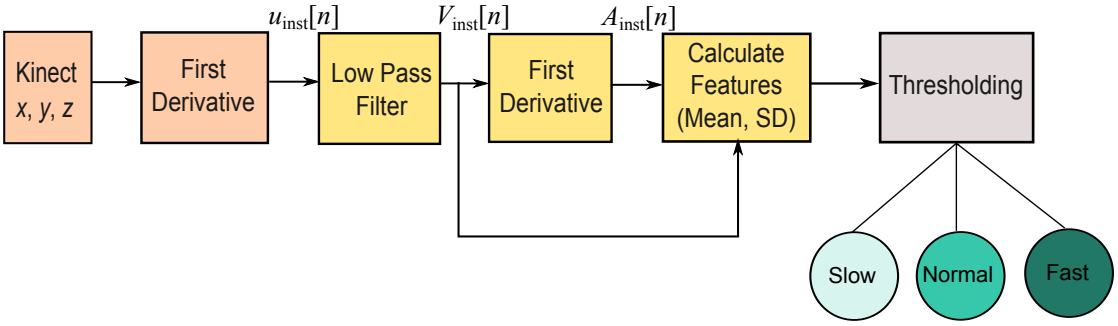

Figure 3: **Flowchart for the arm-movement type classification.** This is the proposed algorithm that consists of three main stages: pre-processing (importing Kinect signals and first derivative), feature extraction(lowpass filter, first derivative, and calculating features) and classification (thresholding).

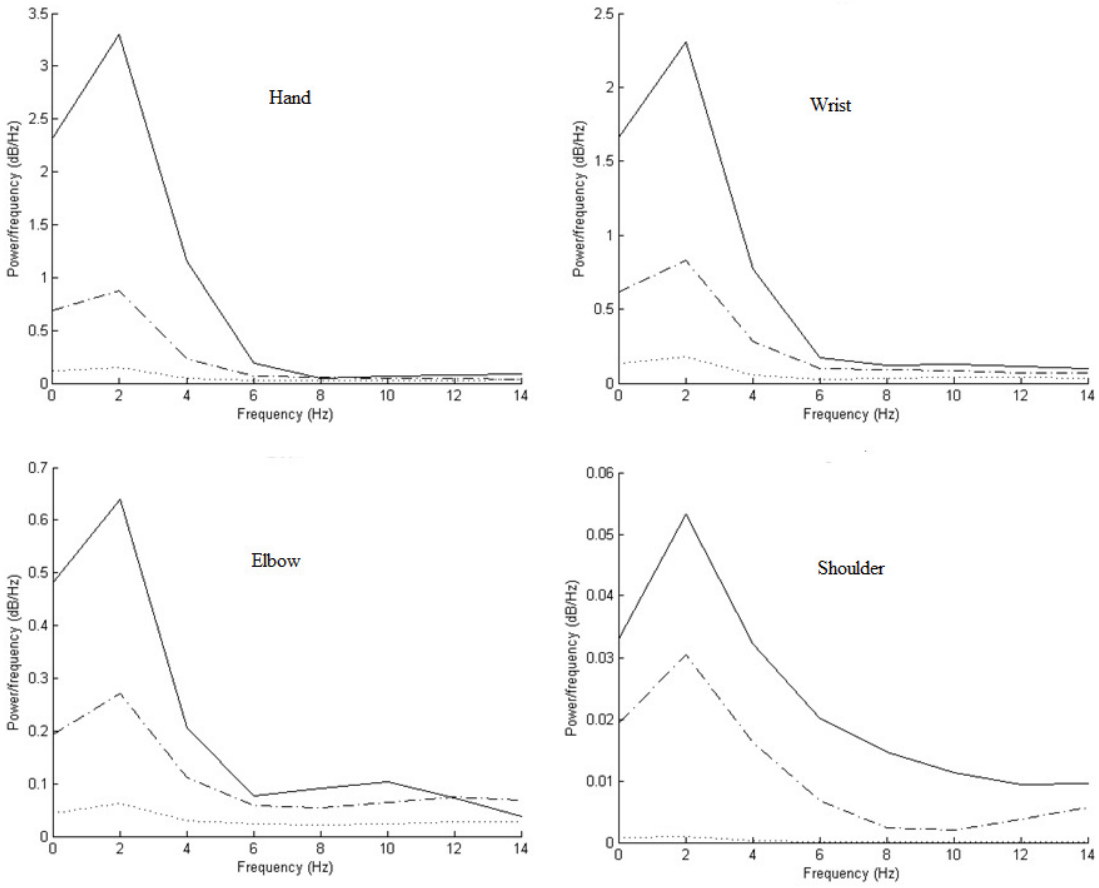

Figure 4: **Power spectra of the three speed motions: slow, normal and fast.** The dotted cureve represents the PSD of a slow hand movement, while the dotted curve cureve represents the PSD of a medium hand movemnt. The PSD of a fast hand movement is the solid curve.

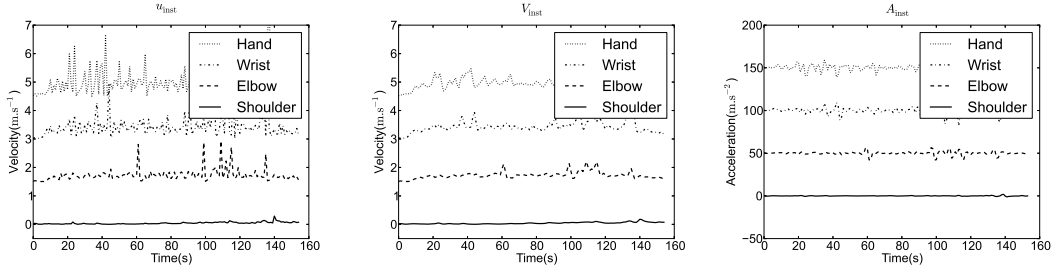

Figure 5: **Comparison of instantaneous velocity and acceleration, non filtered (at left) and filtered (at right) of a slow motion for four joints: shoulder, elbow, wrist and hand of the right arm.** The plots are done for one motion of one subject. For a clearer graph, extra vertical space has been added between the plots, however the scale ratio has been preserved. From bottom to top are shoulder, elbow, wrist and hand respectively. The cutoff frequency of the Butterworth low-pass filter is 6 Hz.

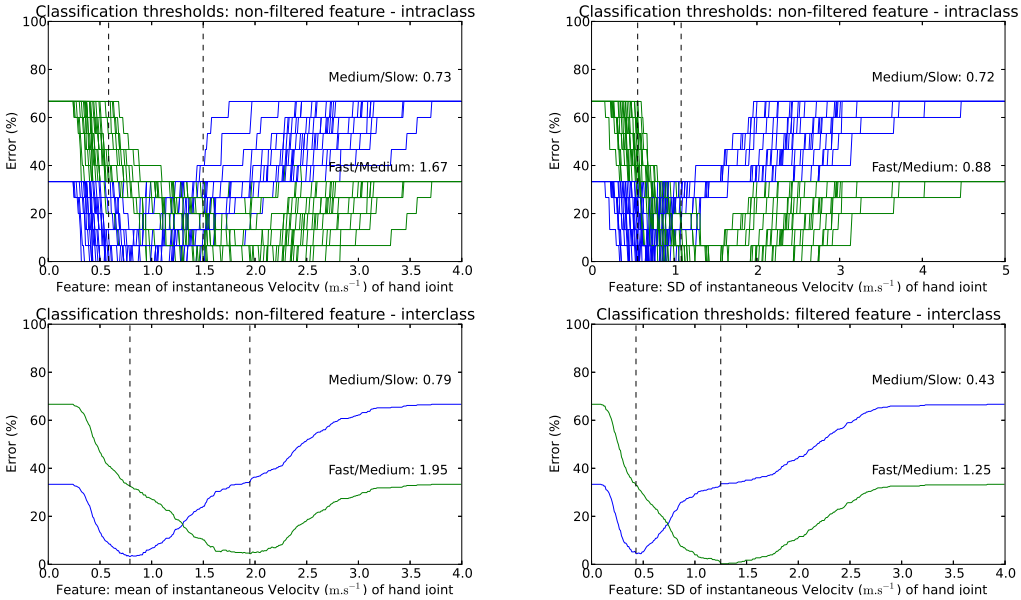

Figure 6: **Threshold of classification.** The top two figures represents the intraclass speed classification for mean and SD, left to right respectively, while the bottom two figures represents the interclass speed classification for the two features: mean and SD of the hand instantaneous velocity. The top two intraclass figures are made by superimposing the figure from each subject and computing thresholds using the average values of each subjects thresholds. The two dashed lines point to the two vallies in figure; and their x-axis values are the used thresholds. The feature at the top-right supposed to filtered SD of the hand instantaneous velocity, however, we demostrated the non-filtered feature as it provides lower error rates based on Table 1.

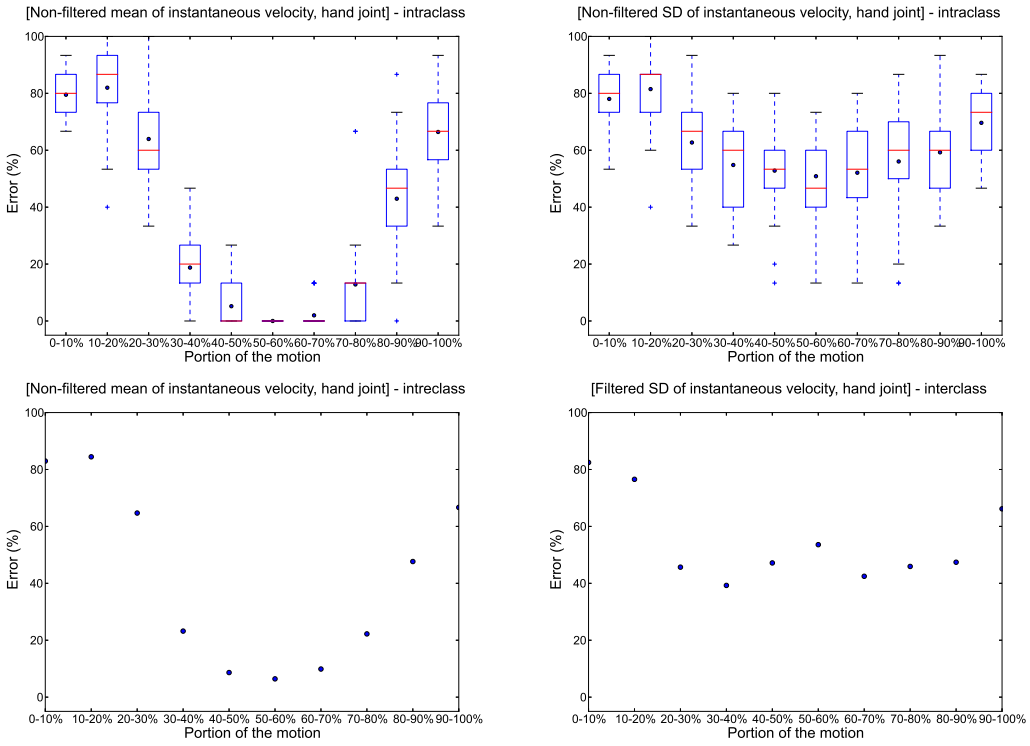

Figure 7: **Classification error rate of the speed types based on the percentage of the whole motion used.** The top two figures represents the intraclass speed classification for mean and SD of the hand instantaneous velocity, left to right respectively, while the bottom two figures represents the interclass speed classification for the same two features (mean and SD). The two intraclass boxplots show the variation within subjects. The two interclass scatters show the exact error rate over all subjects. The portion 0–50% present a comparable error rate to the whole motion. The feature at the top-right supposed to filtered SD of the hand instantaneous velocity, however, we demostrated the non-filtered feature as it provides lower error rates based on Table 1.

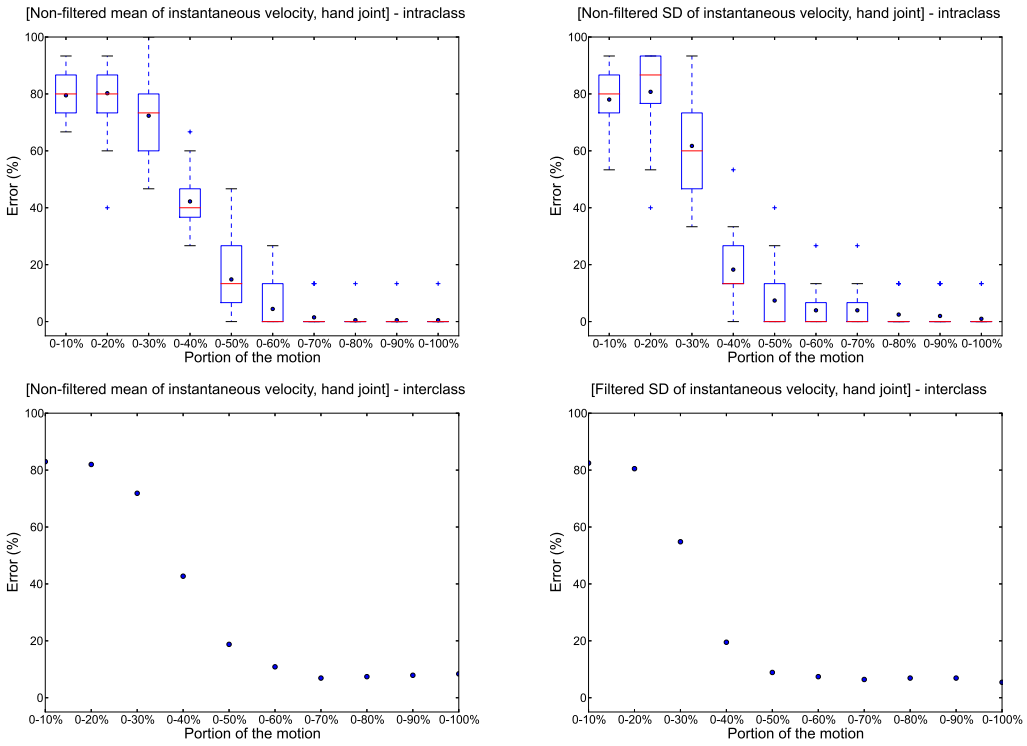

Figure 8: **Classification error rate of the speed types based on a sequential 10% cuts of the whole motion.** The top two figures represents the intraclass speed classification for mean and SD of the hand instantaneous velocity, left to right respectively, while the bottom two figures represents the interclass speed classification for the same two features (mean and SD). The two intraclass boxplots show the variation within subjects, while the two interclass scatters show the exact error rate over all subjects. First we can observe that the classification error diminishes in the middle of the curve, this seems to indicate that the most meaningful section of the motion is at the middle. The smallest error in the portion 50–60% for both intera- and inter- class speed classification. The feature at the top-right supposed to filtered SD of the hand instantaneous velocity, however, we demostrated the non-filtered feature as it provides lower error rates based on Table 1.